ISSN (Print) 1226-1750
ISSN (Online) 2233-6656
Journal of Magnetics 27(2), 164-171 (2022) https://doi.org/10.4283/JMAG.2022.27.2.164

Orthogonal Optimization Design and Finite Element Analysis of Converging Stepped Magnetic Fluid Seal

Fu-xiang Hao and An-le Mu*

School of Mechanical and Precision Instrument Engineering, Xi'an University of Technology, Xi'an 710048, Shaanxi, China

(Received 2 September 2021, Received in final form 23 May 2022, Accepted 23 May 2022)

In order to better solve the problem of air leakage during compressor operation, based on the converging stepped magnetic fluid seal structure, the L_{16} (4^4) orthogonal test design and the numerical simulation of the finite element method are combined to optimize the sealing structure. Four factors, four levels and the corresponding orthogonal table are selected in this paper. The simulation results of each test are calculated and range values are studied. Finally, sealing pressure capability of the structure before and after optimization are calculated and compared. The results show that under the conditions of different axial and radial sealing gaps, the sealing pressure capability of converging stepped magnetic fluid seal structure has been significantly improved after orthogonal optimization, especially when the radial sealing gap is relatively small. The maximum pressure capability can be improved by about 11 %, which fully proves the effectiveness of orthogonal optimization. At the same time, the research results can also provide references for the application of other rotary sealing conditions.

Keywords : compressor, orthogonal optimization test, magnetic fluid seal, converging, finite element analysis

1. Introduction

The compressor is a driven fluid machine, which can lift low pressure air into high pressure air [1, 2]. It has a series of unique advantages, such as simple structure, reliable working performance, and convenient operation. Therefore, it has been widely used in various technological processes such as aerodynamics, refrigeration and air conditioning [3, 4]. It sucks in low-temperature and low-pressure refrigerant from the suction pipe, drives the piston to compress through the operation of the engine, and then pumps high-temperature and high-pressure refrigerant air into the exhaust pipe to provide power for the cooling cycle. There are many factors affecting compressor efficiency, such as serious wear of cylinder and piston ring, which can lead to a significant increase in leakage. Sealing device is the key component of compressors to suppress air leakage, and it directly affects the efficient operation of the unit. Wang *et al.* studied the failure form and contact stress of O-ring seal [5]; M. Fukuta *et al.* analyzed the relationship between leakage and tip seal friction, which laid a foundation for optimizing the parameters of compressors [6]. However, it is difficult to solve this leakage problem by traditional mechanical seal.

Magnetic fluid is a kind of intelligent colloidal fluid, consisting of nano-magnetic particles suspended in the carrier liquid. It not only has the fluidity of liquid, but also has the magnetism of solid materials [7-10]. Magnetic fluid sealing technology is a new type of sealing technology, which has the advantages of zero leakage, long service life, high reliability, good self recovery ability, small torque change and so on. Now it is widely used in aerospace, machinery, petroleum and other fields [11, 12]. When the sealing gap of the compressor shaft is more than 0.3 mm, the sealing pressure capability of the converging stepped magnetic fluid seal structure is better than that of the ordinary magnetic fluid seal structure, Yang *et al.* studied the advancement of this point through theoretical and finite element analysis [13, 14].

Therefore, influences of the height of permanent magnet, number of pole teeth, depth of teeth slots, and width of pole teeth are studied in this paper based on the converging stepped magnetic fluid seal structure and without changing the axial length and outer diameter of the sealing device. The sensitive change range is selected

*Corresponding author: Tel: +86-18049538650
Fax: +18049538650, e-mail: muanle@xaut.edu.cn

and four levels are determined. The research results show that sealing pressure capability after orthogonal optimization has been significantly improved under different axial and radial sealing gaps, especially when the radial sealing gap is relatively small, and the maximum sealing pressure capability can be increased by about 11 %. In this way, the air leakage problem of the compressor in the working process can be solved better. At the same time, the research results can also provide a reference for the application of other rotating sealing conditions.

2. Theoretical Analysis of Magnetic Fluid Seal and Orthogonal Optimization

Generally, the Bernoulli equation of magnetic fluid seal is expressed as [7]:

$$P + \frac{1}{2}\rho_f V^2 + \rho_f gh - \mu_0 \int_0^H M_S dH = C \tag{1}$$

Where P is the pressure of magnetic fluid at a certain position; ρ_f is the density of magnetic fluid; V is the speed of magnetic fluid at a certain position; g is acceleration of gravity; h is the height of the magnetic fluid in a certain position; μ_0 is a permeability of vacuum; M_S is magnetization of magnetic fluid; H is external magnetic field strength; and C is the constant.

For the static pressure in magnetic fluid seals, the influence of velocity on the magnetic fluid seals can be ignored, and the influence of gravity in the sealing gap should also be ignored. Therefore, the total sealing pressure capacity of a magnetic fluid seal can be simplified into the following expression:

$$\Delta P = \mu_0 M_S \sum_{j=1}^{N} (H_{\max}^j - H_{\min}^j) = M_S \sum_{i=j}^{N} (B_{\max}^j - B_{\min}^j) \tag{2}$$

Where $H_{\max}^j$, $H_{\min}^j$, $B_{\max}^j$ and $B_{\min}^j$ are the maximum and minimum magnetic field strengths and the maximum and minimum magnetic flux densities under the *j-th* pole piece, N is the total number of sealing pole pieces.

According to formula (2), we express the total sealing capability of the converging stepped magnetic fluid as [13]:

$$\Delta P_{Totall} \approx M_S \sum_{j=1}^{N} (\Delta B_{ja} + \lambda \Delta B_{jr}) \tag{3}$$

In which ΔB_{ja} and ΔB_{jr} are the difference of magnetic flux densities in the axial and radial sealing gaps formed by the *j-th* pole piece and the converging stepped shaft. When $\Delta B_{ja} < \Delta B_{jr}$, λ=1, otherwise λ=0.

In this paper, the results of orthogonal test are analyzed by range analysis. Range analysis is widely used because of its simple, intuitive and easy to understand [15, 16]. The main theoretical formula are as follows:

$$K_i = \sum_{i=1}^{n} x_i \tag{4}$$

K_i stands for the sum of test indexes when the number of levels is i (i = 1, 2, 3, 4), and x_i is the test result.

$$k_i = \frac{K_i}{r} \tag{5}$$

k_i represents the average value of K_i, and r represents the value at each level on any column.

$$R = \max(K_1, K_2 \ldots K_n) - \min(K_1, K_2 \ldots K_n) \tag{6}$$

R value refers to the difference between the maximum K_i value and minimum K_i value at every level of any series of factors.

3. Structure Design of Converging Stepped Magnetic Fluid Seal

The 2D symmetry structure model of the designed converging stepped magnetic fluid seal with two magnets

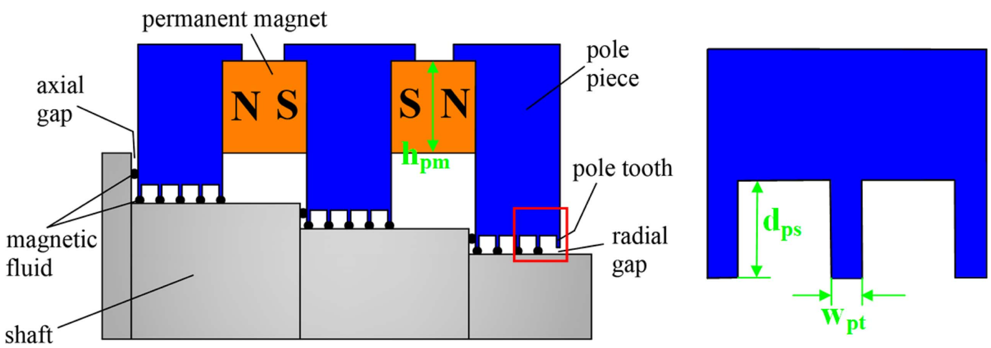

Fig. 1. (Color online) The 2-D structure model of converging stepped magnetic fluid seal (h_{pm} is the height of permanent magnet; d_{ps} is the depth of pole slots; w_{pt} is the width of pole teeth).

Table 1. Parameters of the converging stepped structure in Fig. 1.

Item	Value
Inner radius of the 1/2/3 pole piece (mm)	14.9/18.5/22.1
Outer radius of the 1/2/3 pole piece (mm)	31
Width of the 1/2/3 pole piece (mm)	5
Width of permanent magnets (mm)	5
Inner radius of permanent magnets (mm)	25
Outer radius of permanent magnets (mm)	30
Width of pole teeth (mm)	0.2
Depth of teeth slot (mm)	0.7
Number of pole teeth	5

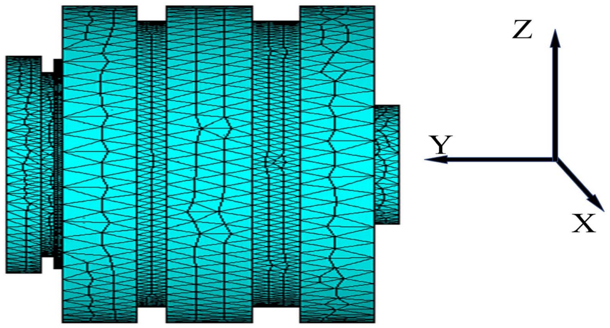

Fig. 2. (Color online) Grid diagram of the three-dimensional model.

is shown in Fig. 1, and its sealing structure magnetic fluid is shown in Table 1.

According to the structural parameters shown in Table 1, model is built in ANSYS software. The material properties of NdFeB are given to the permanent magnets, its coercive force and relative permeability are 1.356×10^6 A/m and 1.05 respectively. The material properties of 2Cr13 are given to the shaft and pole pieces, and the oil-based magnetic fluid with saturation magnetization of 40 kA/m is used. Choosing the intelligent gridding with an

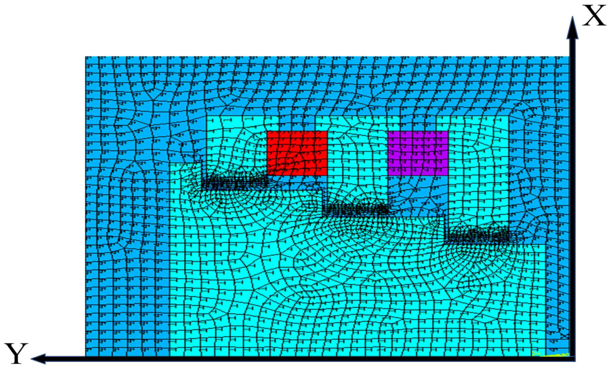

Fig. 3. (Color online) Grid diagram of the two-dimensional model.

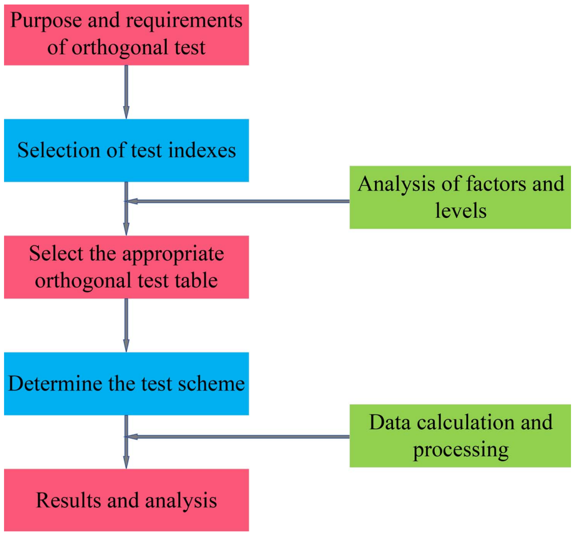

Fig. 4. (Color online) Flow chart of orthogonal test design.

accuracy of 1. The grid diagram of the three-dimensional model of the converging stepped magnetic fluid seal structure is as shown in the Fig. 2. Because the structure is symmetrical about Y axis, it can be simplified to a two-dimensional model, as shown in Fig. 3. The boundary conditions ensures that the magnetic lines of force are parallel to the boundary of the model, which is finally solved by the solver.

4. Orthogonal Optimization Design of Converging Stepped Magnetic Fluid Seal

The variable performance of converging stepped magnetic fluid seal is the result of comprehensive influence of various factors, there are some limitations in changing only a single factor to analyze. In order to make the test design more scientific, we should comprehensively analyze the influence of various factors and levels on the sealing performance. Therefore, the orthogonal test method is used for multi-factor and multi-level number analysis in this paper, and the main design flow chart is shown in Fig. 4.

Table 2. Variable value of sealing conditions and structural parameters.

Item	Value
Axial sealing gap g_a (mm)	0.4
Radial sealing gap g_r (mm)	0.4
Height of permanent magnet h_{pm} (mm)	4.0/4.5/5.0/5.5/6.0/6.5
Number of pole teeth n_{pt}	3/4/5/6/7
Depth of teeth slot d_{ts} (mm)	0.3/0.5/0.7/0.9/1.1
Width of pole teeth w_{pt} (mm)	0.10/0.15/0.20/0.25/0.30

4.1. Purpose and requirement of orthogonal test

The purpose of orthogonal test is to better solve the air leakage problem of the compressor during operation, and to find the optimal structure size of the device. The requirement is to improve the sealing pressure capability of the converging stepped structure under the condition of different axial gaps and radial gaps.

4.2. Select the factors and levels

Four factors that affect the pressure capability of the converging stepped magnetic fluid seal are selected in this paper: height of permanent magnet, number of pole teeth, depth of pole slots, and width of pole teeth.

When the axial sealing gap and radial sealing gap are both 0.4 mm, the magnetic field with four factors by ANSYS software are analyzed, the variable range of each factor is shown in Table 2, and the magnetic flux density curves are shown in Fig. 5.

It can be seen from Fig. 5(a) that the height of the permanent magnet increases, and the corresponding magnetic flux density strength also increases, the reason is that the permanent magnet provide magnetic energy for the whole magnetic circuit as a magnetic source, with the increase of its height, more magnetic energy will be provided for the magnetic circuit. In Fig. 5(b), with the increase of the number of pole teeth, the magnetic flux density in the radial sealing gap will increase, as the number of pole teeth increases, more magnetic induction lines will pass through the radial sealing gap, resulting in an increase in the magnetic flux density in the radial gap. At the same time, it is also found that the magnetic flux density at the radial sealing gap will decrease, because the magnetic energy of the whole magnetic circuit is constant, and the magnetic flux density in the radial sealing gap will increase, which will inevitably lead to the decrease of the magnetic flux density in the axial sealing gap. As can be seen from Fig. 5(c), when the depth of teeth slot is 0.3 mm, the magnetic flux density curve at the radial sealing position is relatively flat and the magnetic induction gradient difference is relatively large, and when the depth of teeth slot is 1.1 mm, the magnetic flux density curve at the radial sealing position is relatively steep, because the larger the depth of teeth slot is, the larger the corresponding magnetic flux density gradient difference

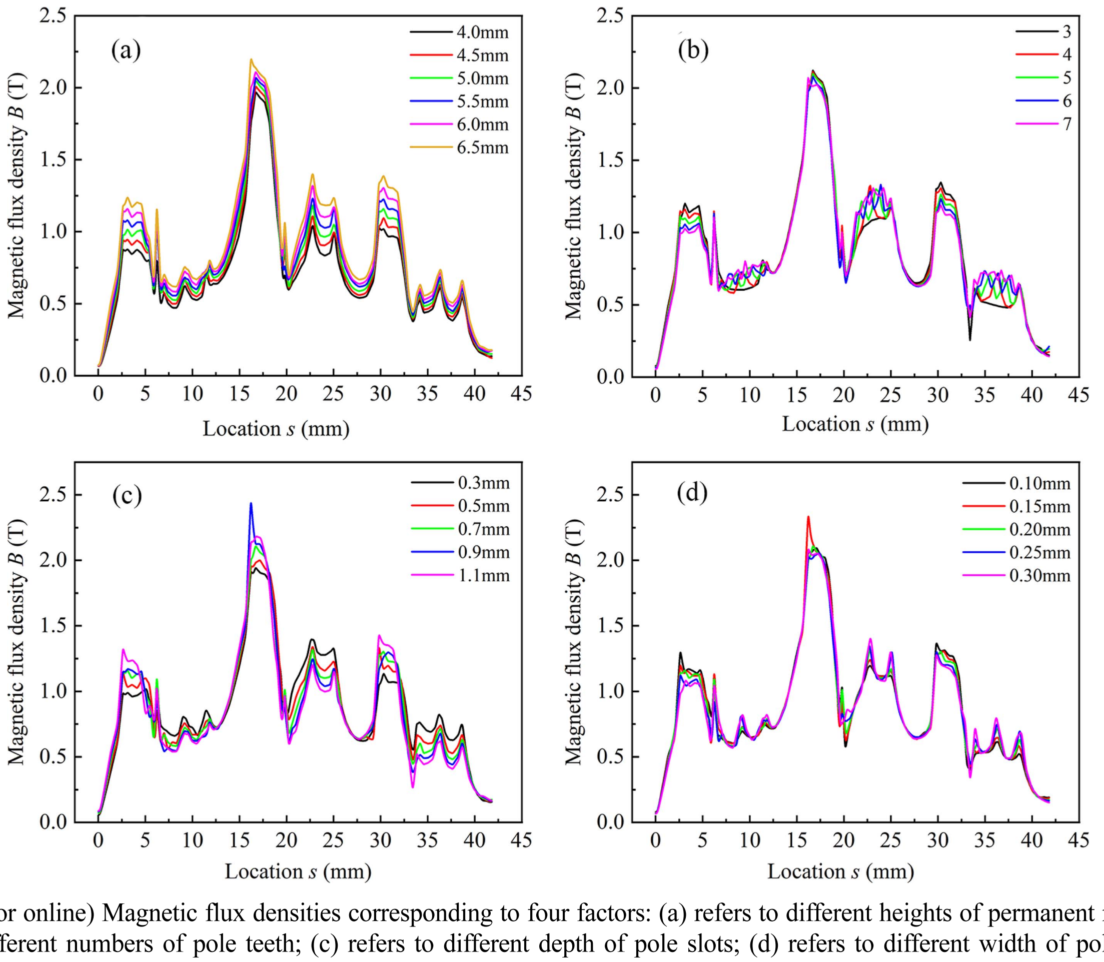

Fig. 5. (Color online) Magnetic flux densities corresponding to four factors: (a) refers to different heights of permanent magnet; (b) refers to different numbers of pole teeth; (c) refers to different depth of pole slots; (d) refers to different width of pole teeth.

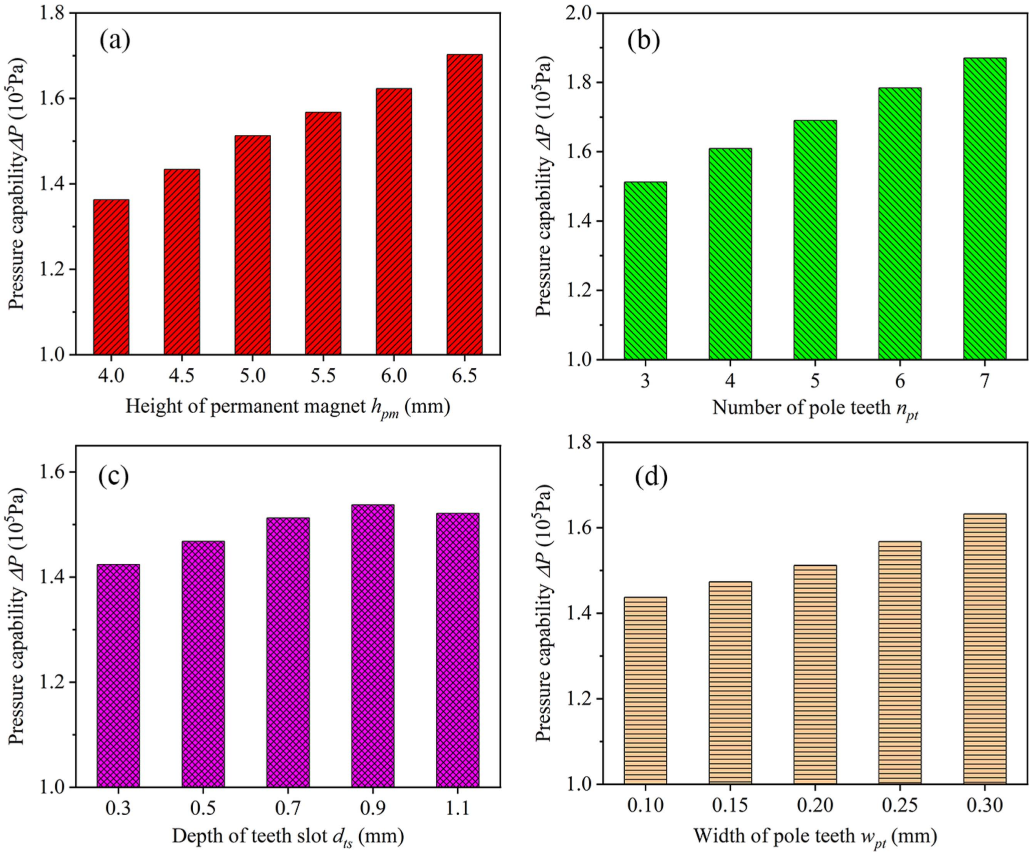

Fig. 6. (Color online) Pressure capabilities corresponding to four factors.

is. It is not difficult to find in Fig. 5(d) that when the width of the pole teeth is 0.3 mm, the magnetic flux density corresponding to the radial position is the largest, because the larger the width of the pole teeth, the more magnetic induction curves will pass, resulting in an increase in magnetic flux density.

According to the magnetic flux density curves corresponding to Fig. 5 and the theoretical formula of magnetic fluid seal, the sealing pressure capability of each factor can be calculated, and the results are shown in Fig. 6.

As can be seen from Fig. 6(a), when the height of permanent magnet is 6.5 mm, the sealing pressure capacity is 1.71 bar, which is the biggest, when the height of permanent magnet is 4 mm, the corresponding sealing pressure capacity is the smallest, which is only 1.363 bar. It can be seen from Fig. 6(b) that with the increase of the number of pole teeth, the sealing pressure capability becomes larger and larger. When the number of pole teeth is 7, the sealing pressure capability can reach 1.861 bar. However, The number of pole teeth can not be too much in the actual machining process, because too many pole teeth will increase the difficulty of machining. As shown in Fig. 6(c), with the increase of depth of pole teeth, the sealing pressure capacity increases firstly and then decreases. When the depth of tooth slot is 0.9 mm, the maximum pressure capability of seal is 1.56 bar, the reason is that when the depth teeth slots is 0.9 mm, the whole magnetic circuit just reaches the maximum magnetic energy product. As can be clearly seen in Fig. 6(d), when the width of the pole teeth is 0.1 mm, the sealing pressure capability is the smallest, which is only 1.43 bar, and when the width of the pole teeth is 0.3 mm, the corresponding sealing pressure capability is the biggest, which is 1.64 bar.

According to the calculation and analysis of the sealing pressure capability value corresponding to the four key factors, the levels of height of permanent magnet are [5.0 mm, 5.5 mm, 6.0 mm, 6.5 mm], the levels of number of pole teeth are [4, 5, 6, 7], the levels depth of teeth slot are [0.5 mm, 0.7 mm, 0.9 mm, 1.1 mm], and the levels of width of pole teeth are [0.15 mm, 0.20 mm, 0.25 mm, 0.30 mm].

4.3. Selection of the appropriate orthogonal test table

The appropriate orthogonal test table is selected

Table 3. Orthogonal test table of factors and levels.

Orthogonal test factors	Symbol	Level 1	Level 2	Level 3	Level 4
Height of permanent magnet h_{pm} (mm)	A	5.0	5.5	6.0	6.5
Number of pole teeth n_{pt}	B	4	5	6	7
Depth of teeth slot d_{ts} (mm)	C	0.5	0.7	0.9	1.1
Width of pole teeth w_{pt} (mm)	D	0.15	0.20	0.25	0.30

according to factors and levels. There are four factors and four levels in this orthogonal test, as shown in Table 3.

In Table 3, the permanent magnet is the magnetic source that provides magnetic energy for the whole magnetic circuit, so the factor of the height of the permanent magnet is put in the first row. Then the number of pole teeth, depth of teeth slots and width of pole teeth are placed in the second row, the third row and the fourth row respectively.

4.4. Determination of the orthogonal test scheme

According to the factors and levels shown in Table 3, the $L_{16}(4^4)$ orthogonal test scheme is established, and the test results are calculated, the results are shown in Table 4. Especially, the interactions between factors are not considered in this design [15, 16].

As shown in Table 4, each test number corresponds to a combined result. Next, range analysis is required.

4.5. Range analysis of orthogonal test

R value reflects the change range of test index when the level of each column of factors changes, the bigger the R value, the greater the impact of this factor on the test index, which proves to be more important. Therefore, according to formula (4), (5), (6) and Table 4, results are calculated and analyzed by using the range analysis method as shown in Table 5.

Table 4. $L_{16}(4^4)$ scheme and calculation results of orthogonal test.

Orthogonal test sequence	Orthogonal test scheme				Test data x_i
	h_{pm} (mm)	n_{pt}	d_{ts} (mm)	w_{pt} (mm)	Pressure capability (10^5 Pa)
1	5.0	4	0.5	0.15	1.5315
2	5.0	5	0.7	0.20	1.6901
3	5.0	6	0.9	0.25	1.8627
4	5.0	7	1.1	0.30	1.9433
5	5.5	4	0.7	0.25	1.7215
6	5.5	5	0.5	0.30	1.8335
7	5.5	6	1.1	0.15	1.8226
8	5.5	7	0.9	0.20	1.9608
9	6.0	4	0.9	0.30	1.8795
10	6.0	5	1.1	0.25	1.8885
11	6.0	6	0.5	0.20	1.8723
12	6.0	7	0.7	0.15	1.9618
13	6.5	4	1.1	0.20	1.7931
14	6.5	5	0.7	0.15	1.8263
15	6.5	6	0.5	0.30	1.9027
16	6.5	7	0.9	0.25	1.9998

Table 5 shows the range analysis of converging stepped

Table 5. Range analysis of orthogonal test.

Test number	Factor A (Height of permanent magnet)	Factor B (Number of pole teeth)	Factor C (Depth of teeth slot)	Factor D (Width of pole teeth)
K_1	7.0176	6.9256	7.1501	7.1385
K_2	7.3384	7.2384	7.1997	7.3163
K_3	7.0621	7.4603	7.6928	7.3754
K_4	7.5719	7.8657	7.4475	7.6561
k_1	1.7569	1.7314	1.7851	1.7846
k_2	1.8346	1.8096	1.7999	1.8291
k_3	1.7655	1.8651	1.9257	1.8438
k_4	1.8804	1.9964	1.8619	1.9141
Range R	0.5543	0.9401	0.5427	0.5176
Optimal order	B>A>C>D			
Optimal level	4	4	3	4
Optimal combination	$A_4B_4C_3D_4$			

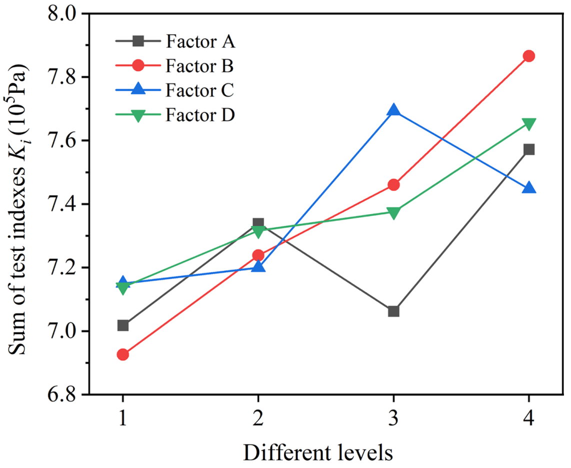

Fig. 7. (Color online) Relationship between different levels and the sum of test indexes.

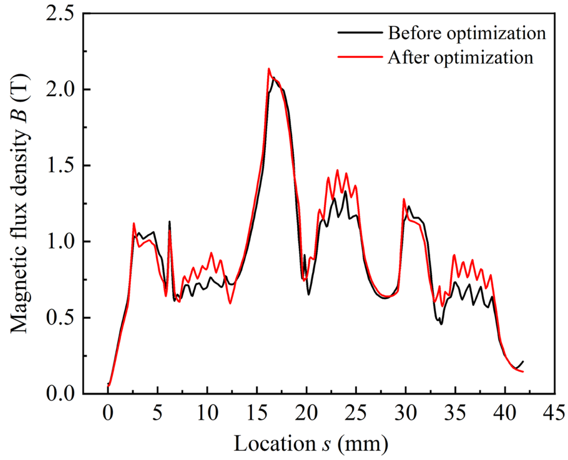

Fig. 8. (Color online) Corresponding magnetic flux density curves before and after optimization: Structural parameters before optimization: h_{pm}=5 mm; n_{pt}=5; d_{ts}=0.7 mm; w_{pt}=0.2 mm; Structural parameters after optimization: h_{pm}=6.5 mm; n_{pt}=7; d_{ts}=0.9 mm; w_{pt}=0.3 mm.

magnetic fluid seal, since the sealing pressure capability is required to be as large as possible, the primary and secondary order of factors can be determined as follows: B(n_{pt}) > A(h_{pm}) > C(d_{ts}) > D(w_{pt}), and the best combination for sealing pressure capability is $A_4B_4C_3D_4$. The sealing pressure capability of the converging stepped magnetic fluid seal structure is the biggest when h_{pm} is 6.5 mm, n_{pt} is 7, d_{ts} is 0.9 mm and w_{pt} is 0.25 mm under other conditions are the same.

In order to better reflect the trend between different levels and the sum of test indexes, the relationship between different levels and K_i is given as shown in Fig. 7.

It can be clearly seen from Fig. 7 that with the increase of factor B and factor D, the sum of test indexes K_i also increase. With the increase of factor A, K_i increased firstly, then decreased and then increased. With the increase of factor C, K_i increased firstly and then decreased.

5. Results and Discussion

Through orthogonal optimization, a new structure is established according to the optimized parameters. When axial sealing gap and radial sealing gap are both 0.4 mm, the magnetic field of the initial structure shown in Table 1 and the optimized structure are analyzed by ANSYS software, and magnetic flux density curves are shown in Fig. 8.

It can be clearly seen in Fig. 8 that the magnetic flux density curve after optimization increases significantly, which proves the effectiveness of the optimal combination in the orthogonal optimization test.

Similarly, the magnetic flux densities of the structure before and after optimization are analyzed in ANSYS software when changing other situations of axial sealing gaps and radial sealing gaps, and sealing pressure capabilities under different sealing gaps before and after optimization are calculated according to formulas (2) and (3), the results are shown in Fig. 9.

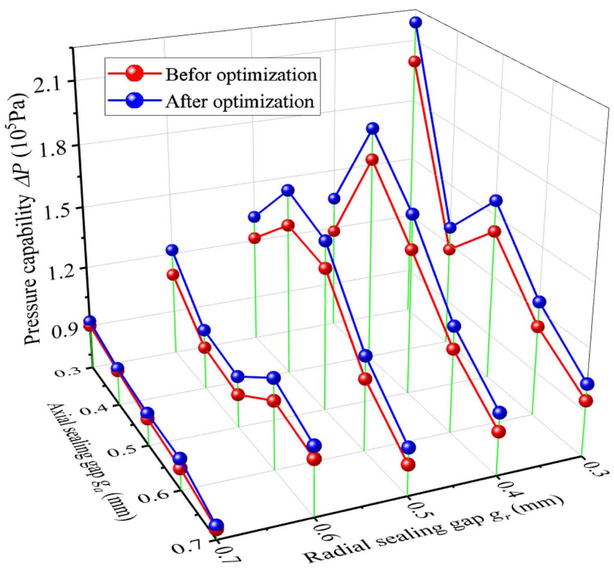

Fig. 9. (Color online) Corresponding sealing pressure capability before and after optimization.

It can be seen from Fig. 9 that the sealing pressure capabilities after optimization have been obviously improved, especially when the radial sealing gap is relatively small, the maximum pressure capability of magnetic fluid seal can be improved by about 11 %. It can also be seen in Fig. 9 that when the radial sealing gap is 0.3 mm and the axial sealing gap is 0.4 mm, the pressure capability of the magnetic fluid seal has been decreased, this is because the sum of the magnetic flux density gradient differences in the axial sealing gap is bigger than the sum of magnetic flux density gradient differences in the radial sealing gap, according to formula (3), the total seal pressure capability is the sum of the pressure capabilities in the axial sealing gaps. Similarly, when the radial sealing gap is 0.4 mm, the axial sealing gap is 0.3 mm, and the radial sealing gap is 0.5 mm, the axial sealing gap is 0.3 mm, the reason is the same. Therefore, the results shown in Fig. 9 prove the effectiveness of the orthogonal optimization.

6. Conclusion

The purpose in this paper is to better solve the problem of air leakage during compressor operation, the structure of converging stepped magnetic fluid seal is optimized by orthogonal test design. On the premise of not changing the axial length and diameter of the sealing device, the four key factors: height of permanent magnet, number of pole teeth, depth of teeth slots and width of pole teeth, are analyzed, and the levels corresponding to each factor are selected. Through the range analysis of orthogonal test, the optimal order is B(n_{pt}) > A(h_{pm}) > C(d_{ts}) > D(w_{pt}), and the optimal combination is $A_4B_4C_3D_4$. The sealing pressure capability of the converging stepped magnetic fluid seal structure is the biggest when h_{pm} is 6.5 mm, n_{pt} is 7, d_{ts} is 0.9 mm and w_{pt} is 0.25 mm under other conditions are the same. The magnetic fields are analyzed and the sealing pressure capabilities are calculated and compared, the results show that sealing pressure capabilities after optimization has been obviously improved, especially when the radial sealing gap is relatively small, the maximum pressure capability of magnetic fluid seal can be improved by about 11 %. This fully proves the effectiveness of orthogonal optimization, at the same time, the research results can provide references for the application of other rotary sealing conditions.

Acknowledgements

The authors thank the National Natural Science Foundation of China (No. 51075326) for providing funding support for this work.

References

[1] X. Meng, Z. Zhang, and X. Li, P. I. Mech. Eng. E-J. Pro. **235**, 1157 (2021).
[2] S. Yamamoto, K. Araki, S. Moriguchi, and *et al.*, Int. J. Heat Mass Tran. **178**, 1 (2021).
[3] D. Hu, L. Yang, and F. Yi, Int. J. Hydrogen Energ. **46**, 27183 (2021) .
[4] D. Liang, D. Jin, and X. Gui, Applied Sciences **11**, 1 (2021).
[5] C. Wang, Z. Xing, S. Sun, and Z. Yu, Cryogenics **166** (2020).
[6] M. Fukuta, T. Sotani, and M. Motozawa, Int. J. Refrigeration **125**, 104 (2021).
[7] D. Li, Beijing: Science Press 232 (2010). (in Chinese).
[8] H. Wang, Ph.D. Dissertation, Beijing Jiaotong University, China, (2018).
[9] Y. Chen, D. Li, Z. Li, and Y. Zhang, IEEE Trans. Magn. **55** (2019).
[10] X. Yang, F. Hao, W. Xu, and *et al.*, Int. J. Applied Electro. Mechanics **60**, 327 (2019).
[11] A. Radionov, A. Podoltsev, and A. Zahorulko, Procedia Engineering **39**, 317 (2012).
[12] H. Zhou, Y. Chen, Y. Zhang, and D. Li, Tribology Tran. **64**, 31 (2021).
[13] X. Yang, P. Sun, F. Chen, F. Hao, and D. Li, IEEE Trans. Magn. **55**, 3 (2019).
[14] F. Chen, X. Yang, S. Gao, and Y. Chen, Inter. J. Applied Electro. and Mechanics **58**, 471 (2018).
[15] J. Wang, C. Men, W. Zhao, and *et al.*, J. Mechanical Engineering **57**, 108 (2021).
[16] Y. Wang and S. Sui, Tsinghua University Press, Beijing, (2017).